PROCEEDINGS OF SCIENCE

Characterization of Atmosphere-Skimming Cosmic-Ray Showers in High-Altitude Balloon-Borne Experiments.

Matias Tueros,[a,*] **Sergio Cabana Freire**[b] **and Jaime Alvarez Muñiz**[b]

[a] *Instituto de Fisica La Plata, CONICET-UNLP, Diagonal 113 entre 63 y 64 , La Plata, Argentina*

[b] *Instituto Galego de Física de Altas Enerxías (IGFAE), Universidade de Santiago de Compostela, 15782 Santiago de Compostela, Spain*

E-mail: tueros@fisica.unlp.edu.ar, sergio.cabana.freire@usc.es, jaime.alvarez@usc.es

Atmosphere-skimming showers are initiated by cosmic rays with an incoming direction such that the full development of the cascade occurs inside the atmosphere without reaching the ground. This new class of showers has been observed in balloon-borne experiments such as ANITA, but a characterisation of their properties is lacking. In this article, we have performed simulations of atmospheric-skimming showers using the latest version of the ZHAireS-RASPASS shower simulation program. We have determined the properties of the longitudinal profile of the shower and its fluctuations as a function of cosmic-ray energy, direction and primary mass. We have studied the phase-space of cosmic-ray arrival directions where detection in balloon-borne experiments is more likely, and have found that only in a small range of directions, the showers are sufficiently developed before reaching the altitude of the detector. The interplay between the Earth's magnetic field, the long distances over which atmosphere-skimming showers develop, and the low density of the atmosphere they traverse gives rise to several effects that are not seen in downward-going cascades. Our results are relevant for the design of balloon-borne experiments and the interpretation of the data they collect.

38th International Cosmic Ray Conference (ICRC2023)
26 July - 3 Aug 2023
Nagoya, Japan

ICRC2023
38th International Cosmic Ray Conference
The Astroparticle Physics Conference

*Speaker

PoS(ICRC2023)348

1. Introduction.

Atmosphere-Skimming or *stratospheric* showers are particle cascades initiated in the atmosphere by primary cosmic rays (and potentially by neutrinos and/or photons) whose incoming trajectories do not intersect the surface of the Earth. They constitute a new class of events first identified in radio pulses collected with the ANITA balloon-borne experiment [1]. In the four independent ANITA flights above Antarctica, 7 *above horizon* events have been detected whose reconstructed zenith angles as seen from an altitude of $\simeq$ 35 km were compatible with showers crossing the atmosphere of the Earth with no core on the ground[1]. The observed pulse properties were in agreement with those expected from showers developing in air and emitting radiation in the MHz - GHz frequency range through the so-called geomagnetic mechanism. The detected pulses showed the expected almost linearly polarized electric field in the direction perpendicular to the magnetic field of the Earth. However, due to the lack of dedicated simulations of these events their energy could not be reconstructed. This type of shower can potentially be detected in other balloon-borne detectors in the planning such as PUEO [2] and EUSO-SPB [3], in satellite-borne experiments like POEMMA [4], and in ground-based observatories such as the Pierre Auger Observatory using the fluorescence detectors [5].

In this work, we present the first simulations of these events using the RASPASS simulation code described in Section 2. Here we concentrate on a characterisation of the longitudinal profile and other properties of the showers that are relevant for radio emission (Section 4). We defer the study of the induced radio emission to an accompanying contribution [6].

2. Simulation of Atmosphere-Skimming showers

In Fig. 1 we show a sketch of an Atmosphere-skimming (AS) shower. The geometry of this type of events can be characterized solely by the minimum distance between the shower trajectory and the Earth's surface (the shower "impact parameter" b).

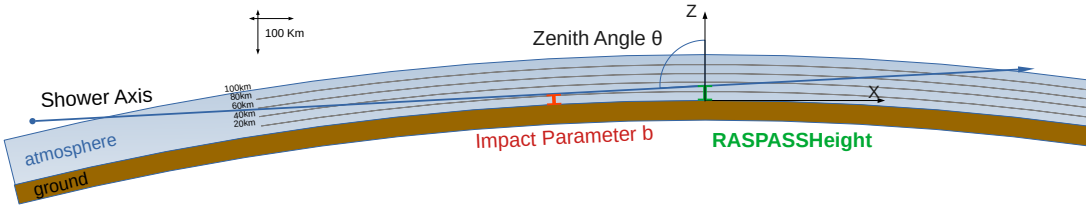

Figure 1: Geometry of an atmosphere-skimming shower with impact parameter $b = 27,2$ km, corresponding to 93° zenith angle. The shower axis crosses the z-coordinate axis at 36 km altitude (`RASPASSHeight`). Earth's curvature is actually shown to scale.

For small impact parameters (b) the shower starts developing in a region of low air density into a zone of higher density, as in the case of a regular downward-going shower. If b is large enough (see Section 4), the shower can further develop in a region of the atmosphere where the density is decreasing again. In any case, and for large enough b, the shower propagates in a very rarefied atmosphere compared to that at ground, resulting in a particle cascade that spreads along the shower

[1] ANITA I, II, III and IV detected 2, 1, 2 and 2 events respectively.

axis over several hundred kilometers, that can escape the atmosphere, and that has ample distance for the Earth's magnetic field to deflect the particles in the low-density atmosphere creating a significant charge separation. Little progress has been done in understanding the influence that the combination of the peculiar geometry and magnetic field can have on the properties of AS cascades and that would influence their detection with radio, fluorescence and/or Cherenkov radiation. Detailed Monte Carlo simulations of these type of events were missing due to the lack of microscopic shower simulation tools capable of handling these geometries until the advent of the ZHAireS-RASPASS program [7] briefly described in the following.

RASPASS stands for **A**ires **S**pecial **P**rimary for **A**tmospheric **S**kimming **S**howers. RASPASS was initially developed in 2011 as a module to simulate *special* primary particles with the shower Monte Carlo simulation program Aires [8], motivated by the first ANITA above-horizon events detected. Later, it evolved into a stand-alone version of ZHAireS [9] (Aires with radio emission calculation capabilities), and it now includes several modifications to allow for the simulation of all sorts of shower geometries: downward-going, upward-going, Earth-skimming and atmosphere-skimming. This program (dubbed ZHAireS-RASPASS) features the same physics algorithms as the standard Aires and ZHAireS, the same user-friendly input of Aires, and it adds the capability to simulate showers initiated by multiple primaries (as for example the decay products of a tau decay) in any event geometry. In ZHAireS/Aires, the geometry of a downward-going shower is determined by the shower zenith angle θ defined with respect to a vertical axis located at the shower core position, and by the azimuth angle ϕ. Although, as stated before, the impact parameter b solely determines the geometry of an AS shower, in RASPASS this type of showers are defined with respect to a high-altitude experiment located at a vertical axis that intercepts the surface of the Earth. For this purpose and as shown in Fig. 1, we define the parameters `RASPASSHeight`, that controls the height at which the shower axis intersects the vertical axis, and the zenith angle θ of the shower, defined with respect to the position of the detector as shown in Fig. 1. For AS showers, θ ranges from slightly below $\simeq 90^\circ$ to the angle at which the horizon is seen from the detector at high altitude. For the particular case of the ANITA balloon-borne detector at $h \simeq 36$ km altitude this is $\simeq 96^\circ$. Given the `RASPASSHeight` and θ, the impact paramter b is uniquely determined.

RASPASS inherits some of the approximations used in Aires/ZHAireS. These limitations are easy to overcome at the expense of CPU time. One of the most important ones is the use of a constant magnetic field that does not change in modulus or direction along the shower development. However, calculations done using the IGRF13 [10] model reveal that for the geometries explored in this work, which are especially unfavorable due to the close proximity to the South pole, the changes in the intensity of the magnetic force are less than 15% along the development of the cascade, and the change in the geomagnetic angle is less than 10°. For this reason, we will consider this approximation good enough to study the general characteristics of AS showers.

3. Relevant phase space for AS showers in balloon-borne detectors.

Significant insight into the characteristics of AS showers can be gained even before doing any simulation, by studying the phase-space available for shower development given an atmospheric density model. In Fig. 2 we show the accumulated matter that a shower, starting at the top of the atmosphere, has to cross before reaching the position of the ANITA detector at an altitude of

$h = 36\,\text{km}$. The amount of atmospheric grammage (in g/cm^2) given by the color scale is shown as a function of the distance to the detector, with ANITA located at distance zero by definition. The grammage is shown as a function of the zenith angle θ. For instance, a shower with $\theta = 93°$ enters the atmosphere at a distance to ANITA of $\simeq 1350\,\text{km}$, and has an available amount of matter to develop until reaching ANITA of $\simeq 1500\,\text{g/cm}^2$. The lower limit to the zenith angle is $\theta = 90°$ below which there is barely no atmosphere to develop, and the upper limit is $\theta \simeq 96°$ above which the shower hits ground before reaching ANITA, corresponding to the zenith angle of the horizon as seen from the altitude of ANITA. It is clearly seen in Fig.2 that as the θ increases the shower develops at lower altitudes in the atmosphere, closer to the ground having a smaller impact parameter b shown in the scale of the top x-axis. As a consequence, the total amount of matter available for development increases correspondingly. For instance, for the extreme case of $\theta \simeq 96°$, the impact parameter is $b = 0\,\text{km}$ and there is a total amount of matter of $\simeq 6 \times 10^4\,\text{g/cm}^2$ between the top of the atmosphere and the ANITA balloon.

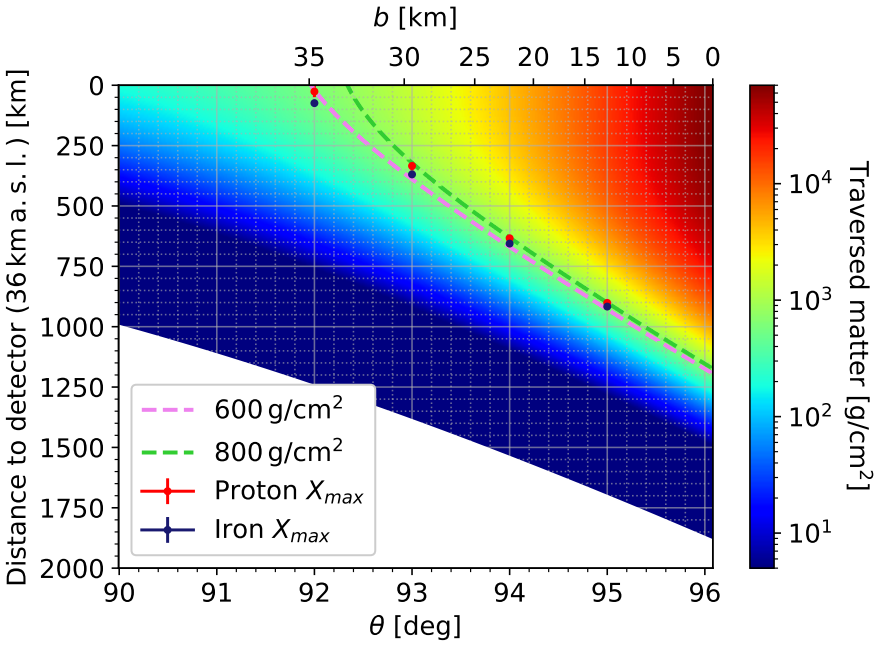

Figure 2: Phase space for the development of atmosphere-skimming air showers passing at an altitude $h = 36\,\text{km}$ height a.s.l. (`RASPASSHeight`= 36 km in Fig. 1). The bottom (top) x-axis represents the shower zenith angle (impact parameter) of the shower. The left y-axis indicates the distance, measured along the shower axis, to the detector. The colour scale represents the traversed matter, along shower axis with a given θ, from the injection point up to a point of the shower axis at a given distance from the detector. The dashed lines show the points where a given slant depth along axis is reached, and the red and blue dots indicate the average X_{max} of $10^{18}\,\text{eV}$ showers.

The dashed lines in Fig. 2 mark the positions along shower axis where an accumulated slant depth of $600\,\text{g/cm}^2$ and $800\,\text{g/cm}^2$ is achieved. These correspond to the typical range of the depth of shower maximum X_{max} for showers at UHE energies. In order to have any sizeable chance of being detected, the shower should develop so that X_{max} is reached before the ANITA detector.

This condition limits the zenith angle range for the relevant AS showers to $92^\circ \lesssim \theta \lesssim 96^\circ$. This favourable zenith-angle window depends on the altitude of the detector and the atmospheric density model. Detectors at higher altitudes will only be able to detect AS events with relatively large θ, as those are the only geometries that will traverse enough matter for the shower to develop. Detectors at lower altitudes have a smaller range in θ where they can see AS events as the angle at which the horizon is located from the point of view of the detector approaches $\theta = 90^\circ$. On the other hand, the probability of seeing more horizontal events and even below $\theta = 90^\circ$ would increase, as now the detector would be in a region with densities high enough to allow for a complete shower development for those angles. The dashed lines in Fig. 2 can also be used to estimate, for each zenith angle, the approximate distance between $X_{\rm max}$ and the ANITA balloon, a parameter that to a large extent determines the attenuation of the radio signal before reaching the detector. Showers with $\theta \simeq 92^\circ$ reach their maximum development at $\simeq 50$ km to the detector, while for $\theta = 96^\circ$ $X_{\rm max}$ typically occurs at about 1200 km. Interference effects, for instance related to seeing the longitudinal development around $X_{\rm max}$ with an observation angle close to the Cherenkov angle in air, also depend largely on this distance. This is discussed in detail in another contribution [6].

4. Phenomenology of Atmosphere-Skimming showers.

The key role played by the density profile of the atmosphere in the development of AS can be studied by fixing `RASPASSHeight`= 36 km to the approximate altitude of ANITA, and simulating showers with $\theta = 92^\circ$, 93° , 94° and 95° corresponding to $b \simeq 32.1$, 27.2 , 20.4 and 11.6 km respectively.

4.1 Longitudinal development

In the left panel of Fig. 3 we show the simulated longitudinal profiles versus the traversed slanted depth (X_s) for iron-induced showers at different θ as obtained with RASPASS. The atmospheric density along the shower axis is also plotted. It is typically more than 1 order of magnitude smaller than the atmospheric density at sea level for these showers developing at a minimum altitude above sea level of $\simeq 11$ km for $\theta < 95^\circ$. The longitudinal shower profiles feature a rather similar shape, independently of θ, when plotted as a function of X_s. The exception are the showers at $\theta = 92^\circ$ that develop in such a rarefied atmosphere that there is not enough matter for the shower to complete its full development before reaching the detector. This was expected in view of the available matter for shower development at $\theta = 92^\circ$ shown in Fig. 2. A clear difference in the maximum number of $e^\pm$, that decreases as θ decreases, can be seen in the left panel of Fig. 3. To understand this, it is important to remember that the longitudinal profile reflects the number of particles crossing planes perpendicular to the shower axis. Due to the bending of charged particle tracks in the magnetic field of the Earth the number of particles crossing a plane perpendicular to shower axis decreases, as the particles propagate along less straight trajectories. This effect is stronger the lower the density, corresponding to showers that develop higher in the atmosphere with smaller θ or larger b. As expected, when artificially turning off the magnetic field in the simulations, the number of particles at maximum is much less dependent on zenith angle as shown in the right panel of Fig. 3.

In Fig. 4 we show the longitudinal development of the number of $e^\pm$ in proton and iron-induced showers at different zenith angles, as a function of the distance to the detector (located at distance

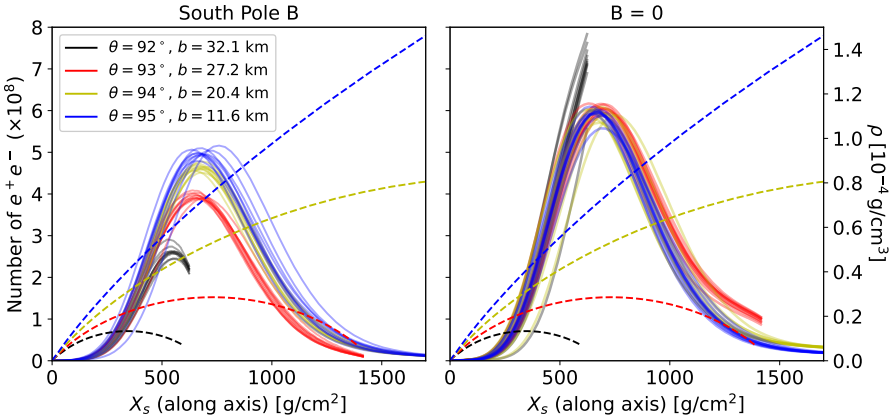

Figure 3: Longitudinal development of ten iron-induced showers of energy 10^{18} eV, for different θ (different impact parameters b), and `RASPASSHeight` = 36 km (see Fig. 1) as obtained with RASPASS. Left panel: Simulations performed with the Earth's magnetic field at the South Pole. Right panel: Magnetic field artificially turned off. Dashed lines (to be read with the right scale of the y-axis) correspond to the density profile along shower axis for each θ.

zero by definition). The strong dependence with θ of the density profile along shower axis (spanning an order of magnitude in the range $\theta = 92°$ to $95°$), is responsible for the large differences in the distance to the detector where the bulk of showers with different θ develop. Showers with θ closer to 90° develop higher in the atmosphere where the density is low and need to travel a larger distance to develop, resulting in wider longitudinal profiles. At the same time, the higher the shower in the atmosphere (or the smaller the value of θ), the smaller is the geometrical distance available between the injection point at the top of the atmosphere and the detector, and as a consequence the showers develop closer to the detector. These features can be seen in Fig. 4.

For showers developing in very low density, event-to-event fluctuations of a few g/cm^2 in the depth of first interaction (X_0) and/or the depth of shower maximum ($X_{\max}$), translate into differences of several tens of kilometers in the distance (relative to the detector) where the bulk of the shower is located. This effect is enhanced the lower the density of the atmosphere, and leads to larger fluctuations in distance for showers with smaller θ as can be seen in Fig. 4. The scale of these fluctuations depends strongly on the density profile along the shower axis, which is itself strongly dependent on θ (dashed lines in Figs. 3 and 4).

4.2 Invisible energy.

The low density in which AS showers propagate represents an unexplored territory for the competition between interaction and decay of hadrons that influences the shower development. In such rarefied atmosphere, the interaction length of hadrons (especially charged pions) will become comparable to its decay length at higher energies than in conventional downward-going showers. Thus, charged pions tend to decay more instead of interacting in a wider energy range, and this reduces the number of hadronic interactions in the shower. As a consequence less neutral pions are produced and the flow of energy towards the electromagnetic component of the shower gets reduced. In turn, the so-called invisible energy, associated to particles that do not deposit the bulk

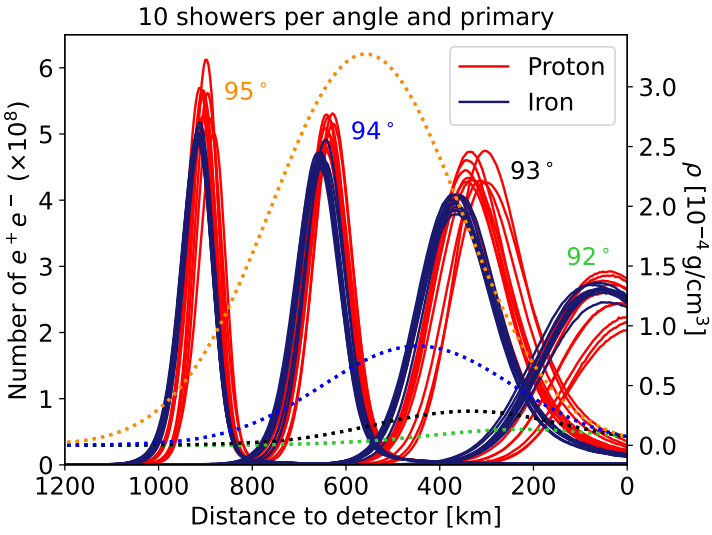

Figure 4: Simulated longitudinal developments of ten proton and ten iron-induced showers of energy 10^{18} eV, for different zenith angles and `RASPASSHeight` = 36 km. The injection point was placed 1650 km away from the $z-$axis in all cases. Dashed lines (to be read with the right scale of the $y-$axis) show the density profiles along shower axis, color-coded to indicate the corresponding zenith angle.

of their energy in the atmosphere, mainly muons and neutrinos, is expected to increase with respect to downward-going showers.

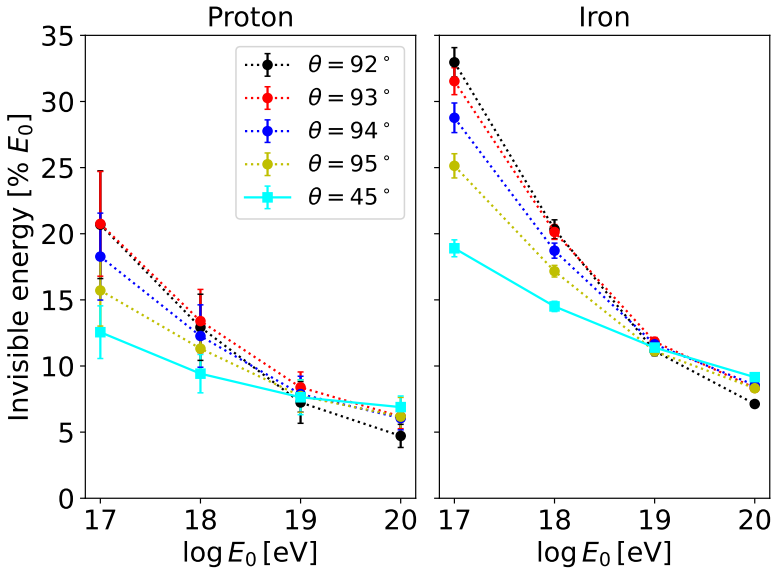

Figure 5: Fraction of invisible energy ($E_{\rm inv}/E_0$) as a function of primary energy E_0, for atmosphere-skimming air showers induced by proton (left) and iron (right) primaries. Each circular marker corresponds to the average of 100 showers simulated with ZHAireS-RASPASS assuming `RASPASSHeight` = 36 km. The cyan squares correspond to the invisible energy estimation in downward-going air showers with $\theta = 45°$.

In Fig. 5, we show the fraction of invisible energy ($E_{\rm inv}/E_0$) as a function of primary energy (E_0) for different θ in p and Fe-induced showers simulated with RASPASS. $E_{\rm inv}$ decreases with E_0 as the number of generations in the shower increases and more π^0s are produced. The trend is similar to that observed in downward-going showers [11]. However, and as expected, $E_{\rm inv}/E_0$ in AS showers is larger than in downward-going showers with the difference decreasing with energy. A special case is that of showers with $\theta = 92^\circ$ and smaller, because at those zenith angles and for a detector at $h = 36\,$km, the shower is not fully developed (Fig. 4). This reduces the number of hadronic generations and also the invisible energy as shown in Fig. 5. As in the case of downward-going showers, $E_{\rm inv}/E_0$ is larger in Fe-induced than in p-induced showers.

5. Conclusion.

The peculiar geometry of atmosphere-skimming air showers gives rise to important differences with respect to downward-going showers, due to the low densities in which they develop, also under the effect of Earth's magnetic field. We have performed a first study of the characteristics of atmosphere-skimming showers and its radio emission (in an accompanying contribution), showcasing that detailed studies of these events are now feasible using ZHAireS-RASPASS.

Acknowledgments: This work is funded by Xunta de Galicia (CIGUS Network of Research Centers & Consolidación ED431C-2021/22 and ED431F-2022/15); MCIN/AEI PID2019-105544GB-I00 - Spain; European Union ERDF.

References

[1] R. Prechelt *et al.* Phys. Rev. D **105**, 042001 (2022), and references therein.
[2] Q. Abarr *et al.*, JINST **16** (2021) 08, P08035.
[3] J. Eser *et al.* PoS(ICRC2021)404.
[4] A.V. Olinto et al. JCAP **06**, 007 (2021).
[5] E. De Vito for the Pierre Auger Collab., PoS(ICRC2023).
[6] M.Tueros, S. Cabana Freire, J. Alvarez-Muñiz, PoS(ICRC2023)349.
[7] M. Tueros, PoS(ARENA2022)056.
[8] S. J. Sciutto [arXiv:astro-ph/9911331]; http://aires.fisica.unlp.edu.ar
[9] J. Alvarez-Muñiz *et al.*, Phys. Rev. D **86**, 123007 (2012).
[10] P. Alken et al. , Earth Planets Space **73**, 49 (2021).
[11] Pierre Auger Collaboration. Phys. Rev. D, **100**, 082003 (2019).
[12] C. Meurer et al. Astrophys. Space Sci. Trans. **7**, **183** (2011).
[13] D. Fargion et al. PoS(ICRC2021)1208 and references therein.
[14] F. Schlüter et al., Eur. Phys. J. C **80**, 643 (2020).
[15] Pierre Auger Collab., Sci. Revs. from the end of the world (Argentina) **1**, 4 (2020) 8.
[16] J. Alvarez-Muñiz et al., Sci. China-Phys. Mech. Astron. **63**, 219501 (2020).